2025 IEEE/SICE International Symposium on System Integration (SII)
January 21-24, 2025, Munich, Germany

Analysis, Modeling, and Control of Merging Behavior at Low Speeds

Tatsuya Ishiguro[1], Hiroyuki Okuda[1], Kenta Tominaga[2], and Tatsuya Suzuki[1]

Abstract— **In a merging environment where automatic and manual operations are mixed, it is important for both parties to communicate with each other. While much research has been conducted at high speeds, such as on expressways, little progress has been made at low speeds, such as on ordinary roads. In this presentation, we will experimentally observe the driving characteristics of drivers in right-angle merging at low speeds, and construct a right-angle merging model that takes negotiation into account.**

I. INTRODUCTION

Autonomous driving has attracted attention for reducing traffic accidents and the burden on drivers. While autonomous driving on highways and expressways is gradually becoming more widespread, in urban areas, social implementation is progressing mainly through mobility as a service(MaaS), that provide transportation, such as taxis and buses. These transportation service vehicles typically use the specialized vehicles with clear indication of their autonomy to surrounding traffic participants, and they often require priority from others. On the other hand, there are numerous technical challenges to enabling privately owned vehicles to operate autonomously. It is not expected that all vehicles will be replaced by autonomous vehicles in the short term, so it is necessary to realize autonomous driving in a mixed traffic environment where autonomous and manually driven vehicles coexist. One of the challenges of autonomous driving technology in such situations is the behavior planning of autonomous vehicles, considering interactions and negotiations with surrounding manually driven vehicles. If the interaction is between autonomous vehicles, direct communication such as vehicle-to-vehicle (V2V) communication can be used to directly control the decision-making process with cooperative control [1], [2]. However, when dealing with manually driven vehicles, the system needs to interpret the intentions of the other driver from the information provided by its onboard sensors and execute driving operations accordingly. Particularly, it requires advanced driving intelligence capable of reaching mutual agreements considering the interactions with others and to be considerate and compassionate similar to how human drivers do.

For example, merging in relatively congested situation are typical driving scenes where mutual agreement through interactions with other vehicles is necessary. In the context of merging, vehicles driving on the main road (hereafter, main road vehicles) generally have priority, however, smooth merging is achieved by interpreting the intentions of merging vehicles and making considerate judgments about yielding or proceeding, with respect to traffic etiquette and consideration for others.

Numerous studies have been conducted on the control of autonomous vehicles during parallel merging on expressways. Most of existing researches have focused on determining the speed and merging position of merging vehicles by evaluating physical quantities such as the distance and relative speed to the main road vehicles [3], [4]. While these researches achieve smooth and safe merging, it is necessary to evaluate not only the behavior norms ensuring safety but also human factors such as reliability and comfort of passengers and drivers on board both the autonomous and surrounding vehicles. Therefore, studies on the modeling of human drivers' judgments in merging vehicles [5], [6] and the acceptability of merging vehicles by main road vehicles [7], [8] have been conducted. Using these judgment models, merging vehicle control that enables smoother consensus formation has been proposed [9].

Although studies on very slow merging scenarios in congested environments like general roads have been conducted, most of these focus on parallel merging [10], with little research on right-angle merging. In this study, the slow right-angle merging situation assuming a scenario where the merging vehicle is an autonomous vehicle going out to merge into the main road from the parking lot and the main road vehicles driving on the main road are manually driven. By observing the driving characteristics of the merging driver and analyzing these characteristics, a numerical merging behavior model that can replicate the merging behavior of human drivers is constructed.

II. TARGETING ENVIRONMENT

The environment assumed in this study is shown in Fig. 1. In the target scene, one vehicle, Car M, is going to merge into the main road from parking space where multiple vehicles (referred to as Car 1 to Car 8 in the figure) are continuously driving on the straight road(main lane).

In this paper, we focus on the driving behavior of the merging vehicle Car M. The merging vehicle Car M drives straight to the stop line and then makes a left turn to merge. However, for simplicity, the merging path is fixed during the merging process in this study. The big goal of this study is to consider the driver model of the merging vehicle, Car M, for the automatic control to realize the human-like autonomous vehicle. The main road vehicles which are

*This work was not supported by any organization

[1]T. Ishiguro, H. Okuda, and T. Suzuki are with Department of Mechanical System Engineering, Nagoya University Graduate school, Furo-cho, Chikusa-ku, Nagoya, Aichi, Japan, email: ishiguro.tatsuya.p1@s.mail.nagoya-u.ac.jp

[2]K. Tominaga belongs to the Advanced Technology RD Center at Mitsubishi Electric Corporation

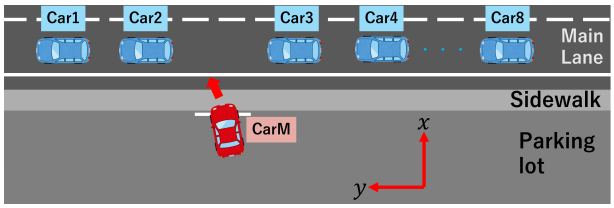

Fig. 1. Target driving environment

Fig. 2. Appearance of Driving Simulator (DS)

considered as manually driven vehicles are automatically controlled individually without any external communication to imitate manual driving in the experiment. In this paper, the observation of driving behavior and simulation are conducted using a driving simulator, and it is assumed that the positions and speeds of all vehicles are observable.

A. Merging behavior observation

In this paper, a merging model based on human behavior data during right-angle merging with extremely slow speed is proposed. At the beginning, a driving behavior measurement using a driving simulator(DS) as shown in Fig. 2 is carried out. The right-angle merging situation from the parking lot environment shown in Fig. 1 was reproduced on the DS. Originally, this experiment aims to observe interactive behaviors, so it would be ideal to conduct behavior observations using a multiplayer simulator where all vehicles are controlled by human drivers. However, in merging scenarios, the merging vehicle interacts with multiple vehicles on the main road, requiring many participants for the experiment. In particular, to observe human-to-human interactions, it is necessary for all vehicles on the main road to be driven by humans, as the timing of the merging vehicle's entry cannot be predicted.

Therefore, this study adopts the following approach:

1) Use simple main road vehicle behavior, have a human operate the merging vehicle, observe its behavior, and model it.
2) Use the constructed merging vehicle model to control the merging vehicle, have a human operate the main road vehicle, observe its behavior, and model it.
3) Use the constructed main road vehicle model to control the merging vehicle, have a human operate the merging vehicle, and observe behavior in an environment where the main road vehicles react to the merging vehicle's actions, then model it.

By repeating steps 2 and 3, this strategy aims to gradually enhance the accuracy of the interactive model and attempt to observe realistic interactions without requiring multiple drivers. In this paper, as the first step, step 1 was conducted, and merging driving experiments were carried out with three subjects. The ethical check by our university was carried out and informed consent was obtained from the subjects before the experiment.

The subjects drove the merging vehicle Car M using the driving simulator and were instructed to merge when they felt they could do so naturally. The main road vehicles are drove with ACC denoted later and 50 experimental scenarios are measured for each subjects.

During the experiment, the following data were observed every 0.01 seconds:

- position, speed, acceleration, and angle of Car M
- position and speed of all main road vehicles
- merging intention of the driver

Here, the merging intention is inherently a psychological internal state and not possible usually to be observed directly. However, for the low-speed merging targeted in this study, it is expected that the timing of the intention and the timing of the action may not necessarily coincide. Therefore, we attempted explicit observation of the subjects' intentions. The moment the subjects changed their intention, that is, made a decision, they were instructed to operate the turn signal and input their intention to merge or wait, which allowed us to explicitly measure the timing of the decision. The decisions were categorized as 'Go', 'Wait', and 'Undecided', defined as follows:

- Go: Input the left turn signal, indicating a definite decision to merge.
- Wait: Input the right turn signal, indicating a decision not to merge.
- Undecided: Yet to input the turn signal, indicating the state before making any decisions.

Note that the driving environment assumes left-hand driving as in Japan and car M are going to merge to left in tested scenario, then the left turn signal is natural to indicate the "Go" intention to merge. For simplicity, hereafter, Go, Wait, and Undecided are referred to as G, W, and U, respectively.

B. Driver models of manually driven cars on main road

The main road vehicles are assumed as "manual driven" cars, however, they are controlled by ACC to imitate the human driver in the experiment. The vehicle implementing ACC is referred to as the Ego vehicle, and the vehicle traveling ahead of the Ego vehicle is referred to as the Preceding vehicle. In this ACC, the acceleration required to achieve the target inter-vehicle distance between the Ego vehicle and the Preceding vehicle is calculated by setting the following three parameters:

- δ_{min} : Reference minimal distance
- a : Acceleration time constant factor
- vel_{limit} : Driving speed limit

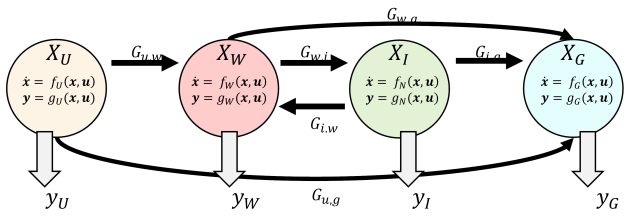

Fig. 3. Proposed merging model

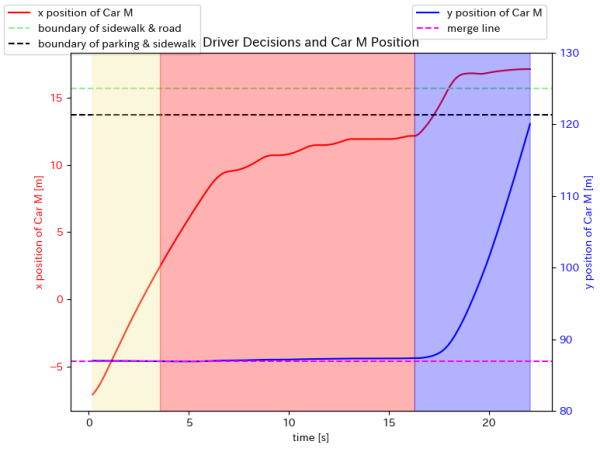

Fig. 4. Relation between driver judgment and position

C. Experimental condition

In this study, to focus on modeling the merging driver's behavior toward the main road vehicles, we primarily set the driving conditions based on the main road vehicles. The driving conditions were set as follows using the parameters described in Section II-B.

- $\delta_{min} \in \{7.5\text{m}, 10\text{m}, 15\text{m}, 20\text{m}, 30\text{m}\}$
- $a \in \{0.6, 0.8, 1.0\}$
- $vel_{limit} \in \{15\text{km/h}, 25\text{km/h}, 35\text{km/h}\}$

A total of 50 driving behavior observation scenarios were created by randomly assigning the above 45 ACC vehicle conditions($5 \times 3 \times 3$) to the 8 main road vehicles.

III. Analysis on Merging Behavior

A. Proposed merging behavior model

Figure 3 shows an overview of the proposed right-angle merging model. This model is divided into four main modes, and transitions between modes occur when the guard function G becomes true. In each mode, a reference speed is output, and the merging vehicle is controlled to follow this reference speed.

- Four modes: The merging characteristics of human drivers obtained from the experimental observation data are classified into four modes. Although the decisions were originally categorized as G, W, and U, a distinctive behavior called 'inching motion: I' was observed within the W category. Therefore, W was divided into W and I, resulting in the four modes: G, W, I, U. Details are described in Section III-C.
- Transition directions from each mode: The transition destinations for each mode are determined based on the observation data. Details are described in Section III-D.
- Guard function: This is composed of mode estimation probability values and a rule-based system. Details are described in Sections IV-A and IV-A.2.
- Output in each mode: The output functions in each mode are determined based on the obtained observation data, and the merging vehicle outputs a reference speed based on the information of the main road vehicles. Details are described in Section IV-B.

B. Analysts on decisions of merging car driver

The data obtained from the experiment is shown in Figure 4. The background colors represent the driver's decisions (blue: G, red: W, yellow: U), with the horizontal axis representing the elapsed time from the start of the scenario and the vertical axis representing the x and y coordinates of Car M as shown in Figure 1.

Focusing on the transition of the x coordinate of Car M, it can be seen that during decision U, the vehicle travels at a constant speed, while during decision W, it decelerates towards the stop line and comes to a stop at the stop line. Subsequently, while still in decision W, the vehicle slightly advances and stops repeatedly, timing its movements before finally transitioning to decision G and merging into the main road. In this study, the behavior of re-accelerating during decision W is defined as 'inching motion (I)'. It is considered that the merging driver approach to main road with slow speed to get ready for the merging by 'inching motion', at the same time, this can be regarded as the implicit communication with the drivers on the road to negotiate their merging order.

C. Data distribution and mode analysis

Within decision W, the re-accelerating and inching forward behavior is considered distinctive and different from the stopping W. Therefore, the observed data obtained based on the acceleration of the merging vehicle $\ddot{x_0}$ and the driver's decision were classified into the following four modes:

- Mode G X_G : Go
- Mode U X_U : Undecided
- Mode W X_W : Wait & $\ddot{x_0} \leq 0$
- Mode I X_I : Wait & $\ddot{x_0} > 0$

Figure 5 shows the data distribution with color coding for each mode. From the figure, it is possible to determine the boundary surfaces of the modes using several combinations of variables.

D. Mode transition and its modeling

Table I summarizes the transition directions between the four modes classified in Section III-C. The data is recorded every 0.01 seconds, with rows representing the mode before the transition and columns representing the mode after the transition. The numbers in the table indicate the count of data for each corresponding transition. Excluding insignificant

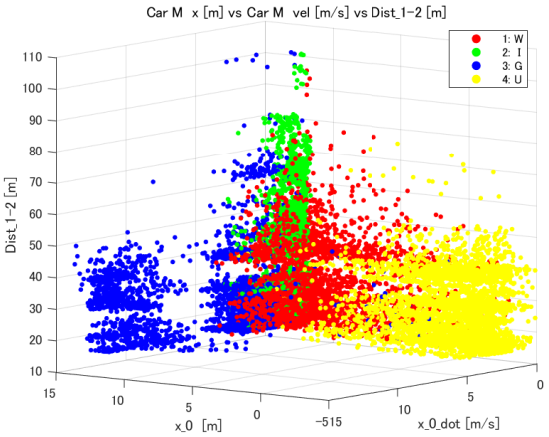

Fig. 5. data distribution

TABLE I
MODE TRANSITION

		To			
		X_U	X_W	X_I	X_G
From	X_U	92673	144	2	12
	X_W	3	226944	1045	47
	X_I	3	969	25548	73
	X_G	6	1	0	64969

transitions due to subject errors, the transitions from each mode are summarized as the hybrid automaton in Fig. 3.

The hybrid automaton in Fig. 3 is formulated as follows:

- Discrete state set :
  $Q = \{X_U, X_W, X_I, X_G\}$
- Output of each state:
  $y_i = g_i(X_i(t), u(t)), \quad i \in \{U, W, I, G\}$
- State transition:
  $$E = \{(X_U, X_U), (X_U, X_W), (X_U, X_G), (X_W, X_W), (X_W, X_I), (X_W, X_G), (X_I, X_I), (X_I, X_W), (X_I, X_G), (X_G, X_G)\}$$
- Guard conditions:
  $G = \{G_{UW}, G_{UG}, G_{WI}, G_{WG}, G_{IW}, G_{IG}\}$
  (details are discussed later)

IV. DETAIL OF MERGING MODEL

A. State transitions

1) State estimation by LRM: In constructing the merging mode estimation model for Car M, a logistic regression model(LRM) was used for the mode estimation. This model allows ambiguous human judgments to be represented probabilistically using a relatively small amount of data. Following explanatory variables are used for the model based on the discussion in the section 5, and shown in Fig. 6.

Explanatory variables of LRM

- $x_0, \dot{x_0}, \ddot{x_0}$: position, velocity, and acceleration of Car M
- $y_1, \dot{y_1}$: y relative position from merging line and driving speed of the nearest car on road

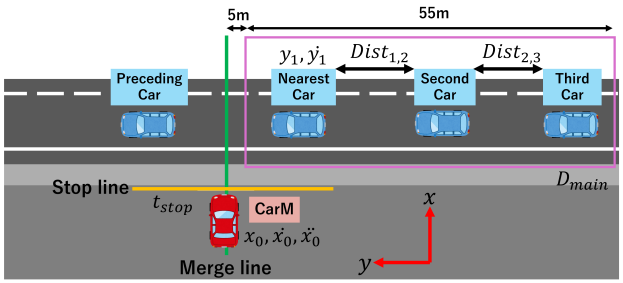

Fig. 6. Definition of each explanatory variable

- $Dist_{1,2}, Dist_{2,3}$: distances from the nearest car and second car, and second car and third car
- t_{stop} : stop duration of car M (the duration while $\dot{x_0} \leq 0.01$m/s, and t_{stop} is reset when $\dot{x_0} > 0.01$)
- D_{main} : Number of mainline vehicles present within 5m to 55m before the Merge line
- ${x_0}^2, {\dot{x_0}}^2, {\ddot{x_0}}^2, {y_1}^2$: square terms of each variables

The explanatory variable vector ϕ is defined as follows:

$$\phi(t) = [1, x_0, \dot{x_0}, \ddot{x_0}, y_1, \dot{y_1}, Dist_{1,2}, Dist_{2,3}, D_{main}, t_{stop}, {x_0}^2, {\dot{x_0}}^2, {\ddot{x_0}}^2, {y_1}^2] \quad (1)$$

Output of LRM The output, resulting variables, of the LRM at the time t is set as follows from the measured data:

1) $X(t) = X_W$: stopping
2) $X(t) = X_I$: inching forward
3) $X(t) = X_G$: go to merge
4) $X(t) = X_U$: undecided

2) Conversion to guard conditions in automaton: Since the LRM estimates the 'stay' probability of each modes, the output probability is converted to the state transition condition. First, the most plausible mode is estimated by taking the highest probability among all modes as follows as the softmax function:

$$\hat{X}(t) = \underset{s}{\operatorname{argmax}}\, P(X(t) = s|\phi(t)) \quad (2)$$

Then, the state transition condition are defined as follows regarding the mode before the transition:

$$G_{ij} = [\hat{X}(t) = X_j] \wedge [X(t-1) = X_i] \quad (i \in \{W, G, I, U\}, j \in \mathcal{F}_i\ ,) \quad (3)$$

where i and j are the states the transition from and to, respectively, and $\mathcal{F}_i$ stands for the set of possible state transition target connected to current state i. For example, the possible mode transitions from X_U are $(X_U, X_U), (X_U, X_W)$, and (X_U, X_G), and the transition from U to W occurs when X_W has the highest probability value among X_U, X_W, and X_G, when the state was U in last time step.

Additionally, to the transition conditions from I mode (G_{IW}) and the transition conditions to G mode (G_{UG}, G_{WG}, G_{IG}), we add rules to replicate the characteristics obtained from observational data and to prohibit merging in ambiguous states (states where the

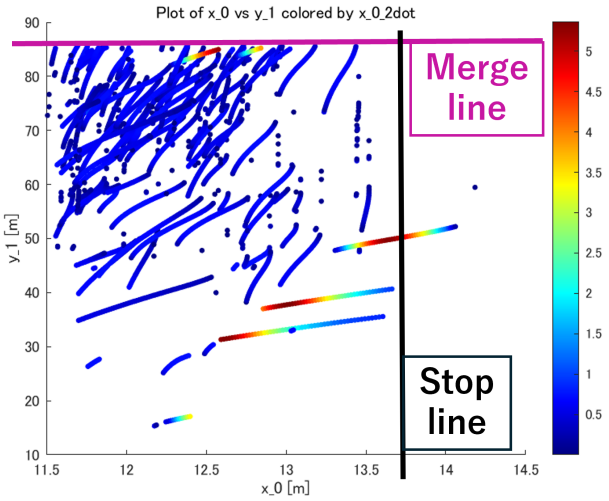

Fig. 7. Inching mode data

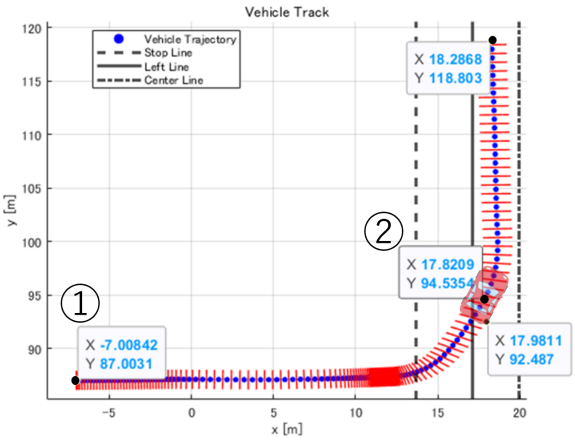

Fig. 8. Merging vehicle travel path

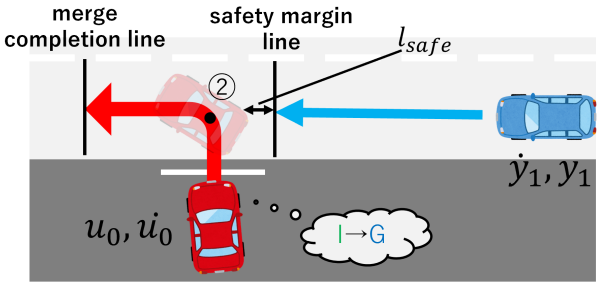

Fig. 9. Variables for collision determination

estimated probability of X_G becomes the maximum by a slight margin).

3) Transition Conditions from I Mode: Extracting only the I mode data from the observational data, Figure 7 shows the nearest vehicle's y coordinate on the vertical axis, the merging vehicle's x coordinate on the horizontal axis, and the merging vehicle's acceleration represented by the color bar. From Fig. 7, it can be observed that the closer the merging vehicle gets to the stop line, the shorter the time it stays in I mode per instance. Therefore, based on the assumption that "the closer to the stop line, the shorter the time a vehicle can stay in I mode," the time the vehicle can stay in I mode, T_I is set as follows using the mean stay time of 0.719 [s] and standard deviation of 0.250 [s]:

$$T_I = -0.704(x_0 - 11.9) + 0.97 \tag{4}$$

The guard function is modified as follows, where $T(X(t))$ represents the time the merging vehicle has continuously remained in I mode.

$$\begin{aligned} G_{IW} =& ([\hat{X}(t) = X_W] \wedge [X(t-1) = X_I]) \\ & \vee [T_I < T(X(t))] \end{aligned} \tag{5}$$

4) Transition Conditions to G Mode: To add a guard condition that prohibits merging which could result in a collision with the nearest vehicle, the transition condition to G mode is updated. Figure 8 shows the merging vehicle's trajectory. The point ① is the starting point of the experimental scenario, and the point ② is the mainline entry point of the merging vehicle. The x, y coordinates and the u coordinate along the path direction for ① and ② are as follows:

- ① : $x_{init} = -7.01,\ y_{init} = 87.0,\ u_{init} = 0.0$
- ② : $x_{in} = 17.8,\ y_{in} = 94.5,\ u_{in} = 29.9$

In Figure 9, let the position and speed of the merging vehicle at the moment when $\hat{X}(t) = X_G$ be u_0 and $\dot{u}_0$, respectively. Assuming the acceleration of the merging vehicle is constant ($a_{merge} = 0.3$G), we calculate the time t_{in} required for the merging vehicle to accelerate to the same speed as the nearest vehicle ($\dot{y}_1$) and then merge at a constant speed until it reaches the mainline entry point (u_{in}). Let the distance traveled while accelerating to $\dot{y}_1$ be u_1. Then:

$$u_1 = \frac{{\dot{y}_1}^2 - {\dot{u}_0}^2}{2a_{merge}}, \quad t_{in} = \frac{\dot{y}_1 - \dot{u}_0}{a_{merge}} + \frac{u_{in} - u_0 - u_{in}}{\dot{y}_1} \tag{6}$$

Additionally, calculating the time t_{main} for the nearest vehicle to reach the safety margin line ($y_{in} - l_{safe}$), we get:

$$t_{main} = \{(y_{in} - l_{safe}) - (y_1 + 2.05)\} / \dot{y}_1 \tag{7}$$

Here, the 2.05 in equation (7) represents the length from the center of gravity to the rear end of the merging vehicle.

Since transitioning to G mode is prohibited in the event of a collision, the condition to prohibit transitioning to G is added as $l_{safe} = 0$ and if $t_{in} \geq t_{main}$. The guard function for transitioning to G is modified as follows:

$$\begin{aligned} G_{iG} =& [\hat{X}(t) = X_G] \wedge [X(t-1) = X_i] \wedge [t_{in} < t_{main}] \\ & \forall i \in \{W, I, U\} \end{aligned} \tag{8}$$

B. Motion models for each mode

Next, the reference speed for each mode is set. The reference speed is also determined based on the observational data.

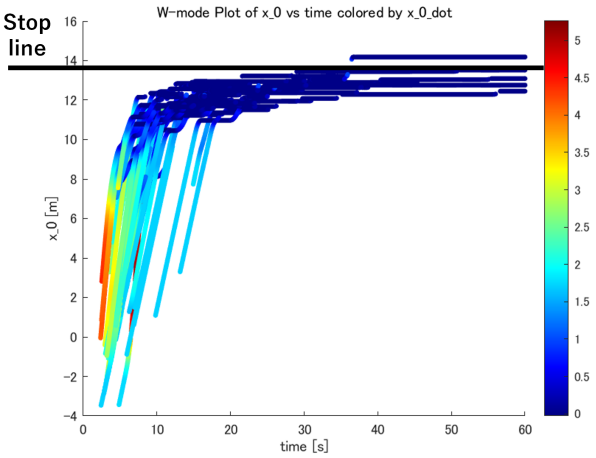

Fig. 10. Driving speed in W mode

1) Reference Speed for U Mode: It was found that the observed data in the X_U state showed almost constant speed driving, so the reference speed in X_U was set to $y_U(t) = 1.95\mathrm{m/s}(= 7.02\mathrm{km/h})$ using the average speed of the merging vehicle in the observed X_U state.

2) Reference Speed for W Mode: 10. The observed data for the X_W state is shown in Figure 10, with the x-coordinate of the merging vehicle on the vertical axis, time on the horizontal axis, and the vehicle's speed represented by the color bar on the right side of the figure. Based on Figure 10, the reference speed $y_W(t)$ in the X_W state was set as follows, to decelerate to 0 m/s by the average stop position at $x = 12.0$ and to continue stopping when $x > 12.0$:

$$y_W(t) = \begin{cases} -0.36(x_0(t) - 12.0) & \text{if} \quad x_0(t) \leq 12.0 \\ 0 \quad \text{if} \quad x_0(t) > 12.0 \end{cases} \tag{9}$$

The average deceleration of $-0.36m/s^2$ from the observed data was used for deceleration.

3) Reference Speed for I Mode: In the data observation experiment, when the merging vehicle engaged in inching, it would release the brake from a stationary state and slowly move forward using the creep phenomenon. To replicate this low speed, the reference speed in the X_I state was set to $y_I(t) = 0.39$ based on the average speed from the observed data. This is combined with the state transition assumption mentioned in Section IV-A.3 that "the closer to the stop line, the shorter the time spent in X_I," to replicate the inching behavior.

4) Reference Speed for G Mode: The reference speed in X_G is set as the safe merging speed calculated at the moment when $\hat{X}(t) = X_G$ (with this time denoted as $t = 0$ in this explanation).

First, for simplicity, the acceleration of the merging vehicle is assumed to change linearly with respect to elapsed time, and is expressed as $a(t) = a_0 + kt$. At this time, the speed and position of the merging vehicle are determined by definite integration as follows:

$$\dot{u}(t) = \dot{u}(0) + a_0 t_{in} + \frac{k{t_{in}}^2}{2} \tag{10}$$

$$u(t) = u(0) + \dot{u}(0)t_{in} + \frac{a_0{t_{in}}^2}{2} + \frac{k{t_{in}}^3}{6} \tag{11}$$

Similar to the approach in Section IV-A.4, for a safe merge, it is necessary to satisfy the following conditions:

$$t_{in} \leq t_{main} \quad and \quad \dot{u}(t_{in}) \geq \dot{y}_1 \tag{12}$$

Here,

$$u(t_{in}) = u_{in} \tag{13}$$

holds true, so using equations (12), (7), and (13), we can derive a_0 and k from equations (10) and (11), and obtain $\dot{u}(t)$ as follows:

$$\dot{u}(t) \geq \dot{u}(0) + a_0 t + kt^2/2 \tag{14}$$

where

$$a_0 = \left(6u_{in} - 6u(0) - \dot{u}(0)t_{in} - 2\dot{y}_1 t_{in}\right)/{t_{in}}^2 \tag{15}$$

$$k = \left(6(2u(0) + \dot{u}t_{in} + \dot{y}_1 t_{in} - 2u_{in})\right)/{t_{in}}^3 \tag{16}$$

$$t_{in} = t_{main} = \left((y_{in} - l_{safe}) - (y_1 + 2.05)\right)/\dot{y}_1 \tag{17}$$

Since the equality in equation (14) represents the lower limit of the driving speed, the reference speed is set to be 2.78 m/s (10 km/h) faster to provide a margin of safety, and is defined as follows:

$$y_G = \dot{u}(0) + a_0 t + kt^2/2 + 2.78 \tag{18}$$

V. Verification in Simulation

A. Experimental conditions for simulations

This chapter describes the simulation verification of the merging model discussed in the previous chapter. Here, the acceleration input is determined using PI control to achieve the reference speed output by the merging model, and the merging vehicle is controlled accordingly. The verification conditions are set to the same 50 conditions as the experimental conditions conducted in Chapter II-A, and the constructed merging model is tested to see if it can replicate human-like merging behavior. When calculating the reference speed y_G, the parameter l_{safe} is set to $l_{safe} = 3.0$, and the upper and lower limits of the merging vehicle's acceleration are set to ± 0.47G based on the observed data. Additionally, after repeated parameter tuning, the PI control gains were implemented as $K_p = 0.5$ and $K_i = 0.1$.

B. simulation results

First, let's discuss the estimation accuracy of the intent estimation model. The observed data were divided into training data and test data. Using the created intent estimation model, the intent for the test data was estimated, and the agreement rate between the actual mode and the estimated mode was calculated, resulting in an average agreement rate of 90.4%. This suggests that the discrete state transitions of the merging model can replicate human intent changes with a certain degree of accuracy.

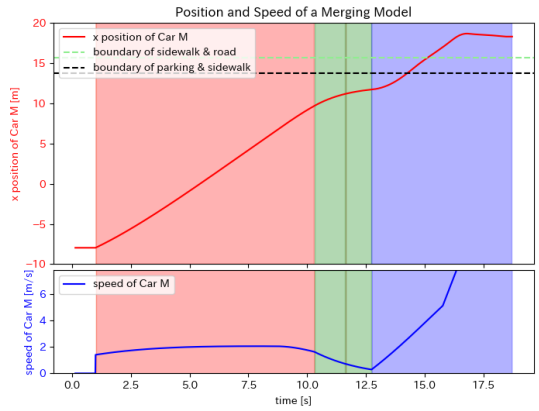

Fig. 11. Vehicle position and speed profiles in simulation

Additionally, Figure 11 shows the x-coordinate and speed profile of the merging vehicle in the simulation. The background color in Figure 11 indicates the state of Car M in the proposed model. It can be seen that the vehicle approaches the stop line in X_W, transitions to X_I while advancing and waiting for the right timing to merge, briefly returns to X_W, and then transitions back to X_I before completing the merge.

The proposed model has confirmed that it can replicate human-like merging behavior, such as inching forward while looking for the right timing to merge, and simultaneously conveying that intent to the mainline driver. However, it is evident that the data for verification in this study is still insufficient, and to thoroughly validate the effectiveness of the proposed model, further verification using observational data from a larger number of drivers is necessary.

VI. Conclusion

In this paper, we aimed to analyze and model human merging behavior at low speed and to achieve right-angle merging control. We proposed a merging behavior model that includes inching motion.

First, the human drivers operations to merge vehicle into main road are measured in driving simulator (DS) to observe their driving behavior and merging intentions. The analysis of the observational data highlighting the inching motion, a state where the vehicle moves forward slowly despite being in a 'wait' state. Based on the hypothesis that this behavior is important for considering interactions with vehicles driving on the road, we constructed a merging behavior model that includes inching motion. Finally, simulations confirmed that the constructed merging model could replicate human-like merging behavior.

In the future, as explained in Chapter II-A, experiments on the main road side will be conducted to build a main road vehicle model. Subsequently, the main road vehicles will be updated, and merging-side experiments will be carried out again. During this process, the number of participants will be increased to construct a merging model that accommodates various driver characteristics.

References

[1] S. Aoki and R. Rajkumar, "V2V-based synchronous intersection protocols for mixed traffic of human-driven and self-driving vehicles," 2019 IEEE 25th International Conference on Embedded and Real-Time Computing Systems and Applications (RTCSA), pp. 1–11, 2019.

[2] Lu, Xiao-Yun and Tan, Han-Shue and Shladover, Steven and Hedrick, J(2004). Automated Vehicle Merging Maneuver Implementation for AHS. Vehicle System Dynamics - VEH SYST DYN. 41. 85-107. 10.1076/vesd.41.2.85.26497.

[3] A. Mosebach, S. Rochner and J. Lunze, "Merging control of cooperative vehicles," IFAC-PapersOnLine, Vol. 49, No. 11, pp.168–174, 2016.

[4] Yasuharu Hayashi, Tohru Namekawa, "Merging Control of Vehicle Platoons Using Distributed Cooperative Model Predictive Control," 60th SICE Annual Conference, November 10, 2017, Tokyo.

[5] Y. Suehiro, T. Wada and Kohei Sonoda, "Assistance Method for Merging by Increasing Clarity of Decision Making," IEEE Transactions on Intelligent Vehicles, Vol.4, No.1, 2019.

[6] C. Dong, J. M. Dolan and B. Litkouhi, "Intention estimation for ramp merging control in autonomous driving," 2017 IEEE Intelligent Vehicles Symposium (IV), Los Angeles, CA, USA, 2017, pp. 1584-1589

[7] Kota Harada, Hiroyuki Okuda, Tatsuya Suzuki, Shintaro Saigo, Satoshi Inoue, "Proposal of a Model Predictive Merging Speed Control Method Considering the Merging Acceptability of Mainline Vehicles," Transactions of the Society of Automotive Engineers of Japan, Vol.49, No.5, September 2018.

[8] R. Otani, Y. Egami, A. Kuriyama, K. Sato and K. Ishii, "Acceptance of Automated Vehicles by Other Drivers during Interaction in Different Motorway Situations" Transactions of the Society of Automotive Engineers of Japan, Vol. 54, No. 2, 2023, pp. 390-395.

[9] H. Okuda, T. Suzuki, K. Harada, S. Saigo and S. Inoue, "Quantitative Driver Acceptance Modeling for Merging Car at Highway Junction and Its Application to the Design of Merging Behavior Control," IEEE Transactions on Intelligent Transportation Systems, No. 1, pp. 329–340, 2019.

[10] Brito, Bruno Ferreira de, Achint Agarwal and Javier Alonso-Mora. "Learning Interaction-aware Guidance Policies for Motion Planning in Dense Traffic Scenarios." ArXiv abs/2107.04538 (2021)